This is the accepted manuscript made available via CHORUS. The article has been published as:

Electric Field Control of the Resistance of Multiferroic Tunnel Junctions with Magnetoelectric Antiferromagnetic Barriers

P. Merodio, A. Kalitsov, M. Chshiev, and J. Velev

Phys. Rev. Applied **5**, 064006 — Published 10 June 2016

DOI: 10.1103/PhysRevApplied.5.064006

Electric field control of the resistance of multiferroic tunnel junctions with magnetoelectric antiferromagnetic barriers

P. Merodio,[1] A. Kalitsov,[1] M. Chshiev,[2] and J. Velev[1,2]

[1]*Department of Physics, University of Puerto Rico, San Juan, Puerto Rico 00931, USA*
[2]*SPINTEC, CEA/CNRS/UJF-Grenoble 1/Grenoble-INP, INAC, 38054 Grenoble, France*

Based on model calculations we predict a magnetoelectric tunneling electroresistance effect in multiferroic tunnel junctions consisting of ferromagnetic electrodes and magnetoelectric antiferromagnetic barriers. Switching of the antiferromagnetic order parameter in the barrier, in applied electric field by means of the magnetoelectric coupling, leads to a substantial change of the resistance of the junction. The effect is explained in terms of the switching of the orientations of local magnetizations at the barrier interfaces affecting the spin-dependent interface transmission probabilities. Magnetoelectric multiferroic materials with finite ferroelectric polarization exhibit an enhanced resistive change due to polarization-induced spin-dependent screening. These results suggest that devices with active barriers based on single-phase magnetoelectric antiferromagnets represent an alternative non-volatile memory concept.

PACS numbers: 85.75.-d, 75.85.+t,77.80.Fm, 73.40.Gk

I. I. INTRODUCTION

Modern spintronics applications, such as field sensing and non-volatile information storage, rely on spin-dependent tunneling in magnetic tunnel junctions (MTJ). The MTJ consists of two ferromagnetic (FM) metal electrodes separated by a thin nonmagnetic insulating barrier. The tunneling current in MTJs depends on the relative orientation of the magnetizations in the electrodes, a phenomenon known as the tunneling magnetoresistance (TMR) effect [1]. The relative orientation between adjacent magnetizations can be controlled by an external magnetic field or a spin-polarized current [2, 3], and the main role of the barrier is *passive*, to separate the magnetic electrodes.

An alternative approach to regulating the tunneling current is the use of *active* barriers possessing internal degrees of freedom that can be controlled separately from the electrodes. In this context, ferroelectric (FE) insulators have emerged as promising candidates for that purpose [4, 5]. The resistive switching element of a FE tunnel junction (FTJ) is a nm-thick FE barrier placed between two non-magnetic metallic electrodes. Here, the electrical resistance change occurs when the electric polarization of the FE barrier is reversed by the application of an external electric field, which gives rise to the tunneling electroresistance (TER) effect [6–10]. If in addition the electrodes are FM metals, the resulting multiferroic tunnel junction (MFTJ) combines both TMR and TER effects, leading to a four-state resistance device that can be used for non-volatile high density memories [11–14].

In single-phase multiferroic (MF) materials the magnetic and ferroelectric orders coexist, which makes them attractive for active barrier applications [15]. The magnetic order in the MF can be FM or antiferromagnetic (AFM). Indeed, MFTJs with FM-MF barriers have already been proposed [16, 17], although the magnetization in the barrier is simply used to replace one of the electrodes. Moreover, there are very few FM-MFs and their excessively low Curie temperatures make them unsuitable for practical applications. At the same time, there are a number of AFM-MF materials with Néel temperatures well above room temperature. These have not been considered for applications because the AFM order parameter is unaffected by magnetic field. Nevertheless, there is class of magnetoelectric (ME) AFM materials, in which the ferroic orders are coupled [18, 19]. The ME coupling can be used to switch the magnetic order parameter by means of an external electric field.

A relatively well-studied example is the prototypical ME material chromia (Cr_2O_3), which exhibits AFM order at room temperature with vanishing zero-field spontaneous polarization [20]. Room temperature ME switching of the AFM order parameter and consequently surface magnetization of chromia have been demonstrated using exchange-biased Cr_2O_3/FM interfaces in the presence of a small symmetry-breaking magnetic field [21, 22]. Recently, magnetization switching by electric field has also been demonstrated in Co thin films exchange coupled to Cr_2O_3 [23]. Moreover, resistance switching has been observed in CrO_2/Cr_2O_3 granular films at some critical voltage, which is consistent with switching of the AFM order in the Cr_2O_3 insulating layer between CrO_2 crystallites via the ME effect [24, 25].

Another example is the prototypical MF material bismuth ferrite ($BiFeO_3$ or BFO). In the bulk, BFO is AFM and FE, but the ME coupling is very small despite its sizable polarization. Nevertheless, in thin film form the ME coupling increases. Indeed, electric field control of the AFM domains in BFO thin films has been shown [26]. Recently, full electric isothermal control of the exchange bias via the ME switching of the AFM order in BFO was demonstrated at low temperature in BFO/FM structures without the aid of external magnetic fields [27, 28]. While ME switching of nm-size ME films is yet to be demonstrated, epitaxial growth of ultrathin ME and MF films is currently a very active and rapidly developing area of

research [29].

Motivated by the aforementioned experimental findings, in this paper we investigate MFTJs with active ME-AFM or ME-MF (FE-AFM) barriers. We demonstrate that the reversal of the AFM order parameter by applied electric field yields a significant change of the tunneling current, representing a ME-enabled TER effect whose origin is markedly distinct from the screening of polarization charges which yields the conventional TER effect. This effect could be at the foundation of a different type of non-volatile voltage-controlled memory element.

II. II. THEORETICAL MODEL

The MFTJ model examined here is illustrated in Fig. 1a. It consists of two semi-infinite FM electrodes separated by a thin ME-AFM or ME-MF (FE-AFM) insulating barrier. The relative orientation of the magnetization in the electrodes can be reversed from parallel (P) to antiparallel (AP) by an applied magnetic field or by spin transfer torque [2, 3] (Fig. 1b). The barrier has AFM order with the local magnetic moments ferromagnetically coupled in the plane and antiferromagnetically coupled between the planes in the direction of the current. The AFM order can be switched by applied electric field as depicted in Fig. 1b. For the ME-MF barrier, we also assume a uniform spontaneous FE polarization perpendicular to the planes [27]. The ferroic orders in the barrier are switched simultaneously by means of an applied voltage pulse (Fig. 1b). From the point of view of our model, it is convenient to think of the ME-AFM and ME-MF cases as identical except for the magnitude of the polarization (zero and finite respectively).

We calculate the tunneling current for the different configurations of the order parameters in the MFTJ using the fully non-collinear non-equilibrium Green's function (NEGF) formalism developed earlier to investigate the transport properties of MFTJs with FE barriers [30, 31]. The electronic structure of the junction is modeled by a single-orbital tight-binding Hamiltonian on a simple cubic lattice in the standard (001) orientation. The lattice constant $a_0 = 2.2$ Å was chosen to be representative of the mean distance between the antiferromagnetically coupled layers in the barrier materials, namely chromia and BFO.

For the electrode material we chose Fe as a typical FM metal. Correspondingly the spin-dependent onsite energies for majority and minority spin channels are set to $\epsilon^{\uparrow} = 2.6$ eV and $\epsilon^{\downarrow} = 4.6$ eV [31]. In the barrier we aim at capturing qualitatively the essential features of the electronic structure in AFM insulators such as chromia and BFO [32, 33]. In both materials the band gap, in the order of a couple of eV, appears between the occupied and the unoccupied 3d orbitals of Cr or Fe respectively. The spin-dependent on-site energies modeling the empty conduction bands here are set at $\epsilon^{\uparrow} = 6$ eV and $\epsilon^{\downarrow} = 7$ eV. We assume that this choice of on-site energies corresponds to a full valence band of majority-spin states producing a net local magnetization pointing in the $-z$ direction. The Fermi level is thus placed close to the middle of the band gap. The nearest-neighbor hopping parameter and Fermi energy at equilibrium are respectively $t = -0.83$ eV and $E_{\rm F} = 0.0$ eV in all regions.

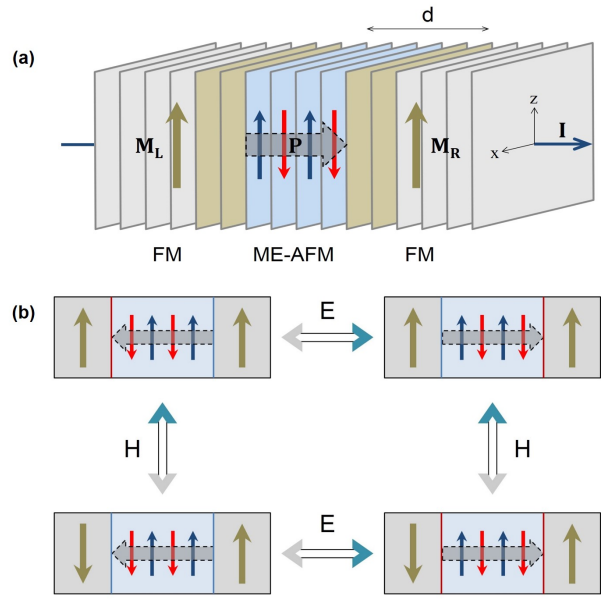

FIG. 1: (a) Schematic diagram of a MFTJ with an active ME-AFM or ME-MF (FE-AFM) barrier. The magnetization $\mathbf{M}_R$ of the right lead is pinned along the $+z$ direction whereas the magnetization $\mathbf{M}_L$ of the left lead can switch between $+z$ and $-z$ (P and AP alignment). When ME-MF barriers are considered, polarization screening takes place within the darker shaded region of the electrode close to the interfaces. (b) Schematic representation of the four configurations that can be adopted by the MFTJ. A magnetic field H can reverse the magnetization in the left lead. The coupled AFM order parameter and polarization P (when it is present) of the barrier can be switched simultaneously by an electric field E due to the ME effect.

The electrostatic potential across the MFTJ is determined in the presence of finite bias and FE polarization by solving Poisson's equation with the following boundary conditions [6, 30, 31, 34]: (i) Constant chemical potentials in the right and left electrodes which are shifted by the applied bias V as $eV = \mu_R - \mu_L$. (ii) Thomas-Fermi screening in the electrodes, where the screening lengths $\lambda_{L/R}$ are determined from the electronic structure. The screening takes place within a few layers from the interface (shaded areas of Fig. 1a). (iii) Polarization-induced bound charges at the interface $\pm\sigma_P = \pm P$. We use a relative permittivity $\epsilon_r = 90$ in the barrier. Chromia exhibits no macroscopic polarization. For BFO we chose $P = 30$ μC/cm^2 which magnitude is representative of perovskite FEs.

Finally the charge current density is calculated using the Keldysh NEGF formalism [35]:

$$I = \frac{et}{8\pi^3\hbar}\int dE d\mathbf{k}_\parallel \mathrm{Tr}[\hat{G}^{<\sigma,\sigma'}_{i+1,i} - \hat{G}^{<\sigma,\sigma'}_{i,i+1}] \quad (1)$$

where $\hat{G}^{<\sigma,\sigma'}_{i,j}$ is the non-equilibrium Green's function correlating the atomic layers i and j. The trace is taken over the spin indices σ and σ' and the integration is performed over the electron's energy and transverse component of the wave vector within the 2D Brillouin zone. All calculations are performed at room temperature.

III. III. RESULTS AND DISCUSSION

A. A. Compensated barriers with vanishing polarization

First we examine the case of FM/ME-AFM/FM MFTJs where the barrier has vanishing macroscopic polarization, representative of the case of a chromia barrier. The crystal structure of Cr_2O_3 consists of Cr-O-Cr trilayers in the (0001) direction where the spins on the two Cr layers are opposite and compensate each other [22]. Consequently the number of magnetic layers in the barriers is always even and the magnetizations at the two interfaces are opposite. Electric-field switching the AFM order parameter in chromia requires a small symmetry-breaking magnetic field H to be applied along with the driving electric field E [21, 22]. However, for ultrathin ME layers the stray magnetic field of the adjacent pinned layer could be sufficient for that purpose [36].

We calculate the I-V curves for the four different configurations shown in Fig. 1b. As a measure of the resistance change, following the ME switching of the AFM order parameter in the barrier for a particular orientation of the magnetizations in the electrodes, we define the ME-TER effect as follows: ME-TER $= (I_{\uparrow..\downarrow} - I_{\downarrow..\uparrow})/(I_{\uparrow..\downarrow} + I_{\downarrow..\uparrow})$, where the arrows denote the AFM order in the barrier (Fig. 1b).

In Fig. 2 the bias dependence of ME-TER for P and AP orientations of the magnetizations in the leads is plotted for barriers containing 2, 4, 6, or 8 magnetic layers. We find that all junctions exhibit ME-TER at finite bias. In the P configuration the ME-TER effect is rather small, less than 2%. Due to the symmetries of the junction, $I_{\uparrow..\downarrow}(-\mathrm{V}) = -I_{\downarrow..\uparrow}(\mathrm{V})$ and $I_{\downarrow..\uparrow}(-\mathrm{V}) = I_{\uparrow..\downarrow}(\mathrm{V})$. Therefore, ME-TER is an odd function of the bias, passing through the origin at zero voltage. In contrast, the AP configuration shows very substantial ME-TER values. In this case, $I_{\uparrow..\downarrow}(-\mathrm{V}) = -I_{\uparrow..\downarrow}(\mathrm{V})$ and $I_{\downarrow..\uparrow}(-\mathrm{V}) = I_{\downarrow..\uparrow}(\mathrm{V})$, hence the ME-TER is an even function of the bias. It does not vanish at zero voltage, but similarly to the P case it increases fairly weakly with the absolute value of the applied bias. The thickness dependence is also very weak, which indicates that for compensated barriers ME-TER is an interfacial effect.

Since the barrier exhibits no net magnetization and no FE polarization, the conventional TER and spin filtering effects are excluded as the origin of the resistance changes. The effect can be understood in terms of interface transmission probabilities [37–39]. If the barrier is sufficiently thick the transmission probability can be written as $T(E, \mathbf{k}_\parallel) = t_L \exp[-2\kappa d] t_R$, where κ is the lowest decay rate for the carriers in the barrier, d is the barrier thickness, and $t_{L/R}$ are the interface transmission functions (ITFs). ITFs can be interpreted as an induced electrode DOS in the barrier. In the P configuration the alignment of local magnetizations at the interfaces is $\uparrow|\uparrow...\downarrow|\uparrow$ or $\uparrow|\downarrow...\uparrow|\uparrow$. In both cases the transmission is proportional to $t^{\uparrow\uparrow}t^{\uparrow\downarrow}$ which makes the currents for the two barrier configurations very similar, leading to a low ME-TER. On the other hand, the magnetization alignment at the interfaces in the AP configuration is $\downarrow|\uparrow...\downarrow|\uparrow$ or $\downarrow|\downarrow...\uparrow|\uparrow$. In the first case the transmission is proportional to $(t^{\downarrow\uparrow})^2$ while in the second is proportional to $(t^{\uparrow\uparrow})^2$. Due to the wavefunction mismatch for the two spins we expect that $|t^{\downarrow\uparrow}| \neq |t^{\uparrow\uparrow}|$, which causes the current in one of the configurations to be higher than the other and correspondingly produces a sizeable ME-TER effect.

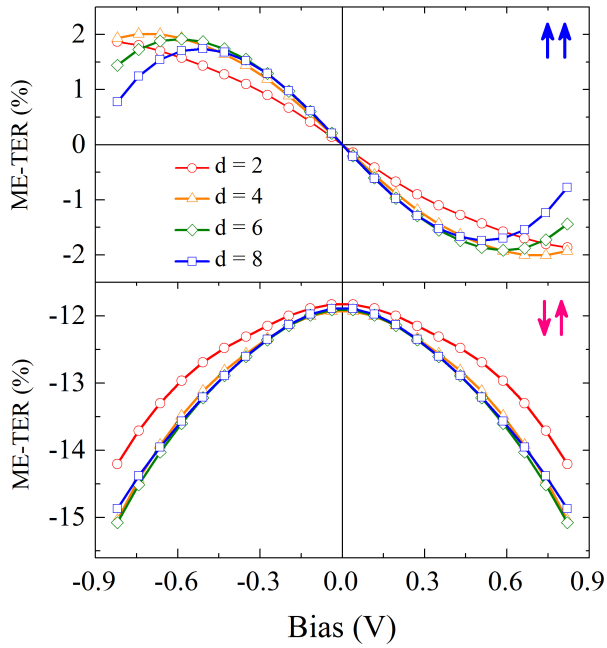

FIG. 2: ME-TER as a function of the bias applied to MFTJs with P (top) and AP (bottom) alignment of the FM electrodes. The number of magnetic layers in the barrier is even and varies from 2 to 8 monolayers (0.44 to 1.76 nm).

Thus we find that MFTJs with ME-AFM barriers exhibit a different kind of electroresistance effect, where the resistance changes purely in response to the switching of the AFM order parameter by electric field via the ME coupling. Despite the fact that the barrier does not have a net magnetization, the switching of the interface magnetization is sufficient to produce a marked difference in the resistance. Moreover, we find a very large tunability

of the ME-TER effect. By switching the mutual orientation of the magnetizations in the electrodes from AP to P the ME-TER effect can be essentially turned on and off.

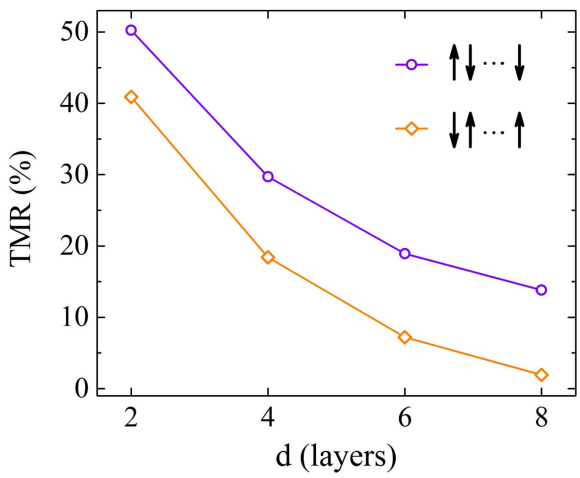

FIG. 3: TMR in MFTJs at zero bias as a function of the barrier thickness d. The magnetization in the left electrode is fixed in the $+z$ direction. The barrier has two distinct magnetic configurations: with the local magnetic moment at the left interface in the $+z$ or in the $-z$ direction respectively. The polarization is set to zero.

Conversely, the magnetization switching in the electrodes is associated with the conventional TMR effect, which can be defined as TMR $= \left(I^P - I^{AP}\right) / \left(I^P + I^{AP}\right)$, where $I^{P/AP}$ designates the current for the P/AP configuration. In Fig. 3 the dependence of TMR on the thickness of the AFM barrier is shown at zero bias. There are four possible magnetic configurations which can be produced by switching the AFM order in the barrier and the magnetic configurations of the electrodes. The P configuration of the electrodes results in equivalent magnetic arrangements for the two AFM states of the barrier, i.e., $\uparrow|\downarrow...\uparrow|\uparrow$ and $\uparrow|\uparrow...\downarrow|\uparrow$. On the contrary, the AP configuration allows for two distinct magnetic alignments, $\downarrow|\downarrow...\uparrow|\uparrow$ and $\downarrow|\uparrow...\downarrow|\uparrow$. Hence, I^P is unaffected by the AFM order switching, but I^{AP} is different for the two AFM states. Consequently the TMR values fall on two distinct curves between which the junction can be switched by applied electric field (Fig. 3). The plot shows quite substantial tunability of TMR by electric switching of the AFM order parameter in the barrier. The coexistence of TMR and ME-TER effects could enable a four-resistive-state functionality for memory applications.

Based on these results, we point out that the characteristic features of the ME-TER effect may have already been experimentally observed in $CrO_2/Cr_2O_3/CrO_2$ junctions [24, 25]. Indeed, the work reported in Ref. [24] demonstrates resistive switching at a threshold voltage applied to CrO_2/Cr_2O_3 granular films where 1-2 nm insulating layers of Cr_2O_3 form spontaneously between CrO_2 FM crystallites. The resulting hysteretic behaviour of the I-V curves was originally ascribed to current-induced switching phenomena, however, the temperature interval in which the effect is present suggests that it is rather associated with ME switching of the chromia AFM order [25]. Moreover, the bistable conductance at zero-bias, the voltage threshold (necessary for the AFM order parameter reversal), and the effect cancellation in the presence of an applied magnetic field (which likely aligns the magnetizations of the CrO_2 crystals in a P configuration), all point to the ME-TER effect.

B. B. Compensated barriers with finite polarization

Next we consider FM/ME-MF/FM MFTJs with a barrier exhibiting AFM order and finite FE polarization, representative of the case of BFO. Due to the polarization, the application of an auxiliary magnetic field is not necessary for switching the AFM order in BFO [40]. We assume compensated magnetization in the barrier, i.e., even number of magnetic layers. The TER effect is now associated with the simultaneous switching of the AFM order parameter and the FE polarization direction: TER $= (I_{\rightarrow,\uparrow..\downarrow} - I_{\leftarrow,\downarrow..\uparrow})/(I_{\rightarrow,\uparrow..\downarrow} + I_{\leftarrow,\downarrow..\uparrow})$, where the horizontal arrows indicate the polarization direction and the vertical the magnetic order in the barrier (Fig. 1b). This represents a generalized electroresistance effect which encapsulates both the ME-TER effect associated with the AFM order switching described earlier and the conventional or FE-TER effect associated with the polarization switching [5].

The bias behavior of the TER for P and AP orientations of the magnetizations in the electrodes is shown in Fig. 4. In the P configuration, the TER is much larger than the ME-TER effect alone. In this configuration both FE-TER and ME-TER have the same parity with respect to voltage, which preserves the shape of the graph and the two effects add constructively. The strong thickness dependence of the FE-TER (not shown) explains the increasing values of TER with the number of magnetic layers, compared to the thickness-insensitive ME-TER (Fig. 2).

Polarization screening gives the dominant contribution to the bias dependence in the AP configuration as well (Fig. 4). The resulting graph is essentially the superposition of the two effects, where the monotonous bias dependence is due to the conventional polarization screening contribution, whereas the offset at zero bias is due to the AFM order switching. The bias asymmetry comes from the different parity of the two effects, even for ME-TER and odd for FE-TER. The generalized TER effect shows lower tunability than ME-TER with switching the magnetic configuration in the electrodes, due to the contribution of the FE-TER effect. Thus for materials with finite polarization the on and off toggling, by switching

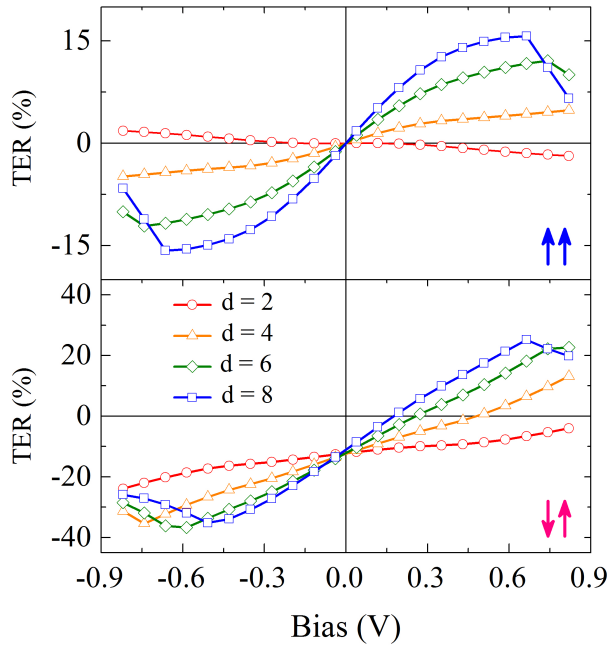

FIG. 4: Bias dependence of TER in MFTJ with P (top) and AP (bottom) alignment of the FM electrodes. The number of magnetic layers in the barrier is even and varies from 2 to 8 monolayers. The FE polarization is set to $P = 30\ \mu\mathrm{C/cm}^2$.

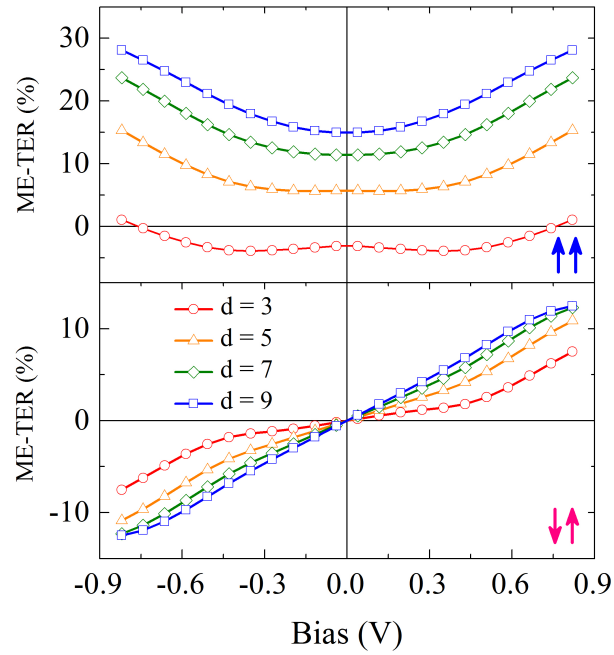

FIG. 5: Bias dependence of ME-TER in MFTJs with P (top) and AP (bottom) alignment of the FM electrodes. The number of magnetic layers in the barrier is odd and ranges from 3 to 9 monolayers. The FE polarization is set to zero.

the magnetic configuration in the electrodes, can only be achieved at low bias. This feature could be used in magneto-transport measurements to experimentally detect the trace of ME-TER effect.

C. C. Uncompensated barriers with vanishing polarization

The structure of chromia is such that the Cr layers come in pairs and there is no net magnetization in the barrier. However, in the case of perovskite ME-MFs, such as BFO, it may be also feasible to grow an odd number of unit cells producing an uncompensated magnetic moment in the barrier. For this reason we consider ME barriers with an odd number of magnetic layers. In order to decouple the different contributions to the TER effect, first we study the case of vanishing FE polarization in the barrier. The bias dependence of the ME-TER effect for the corresponding MFTJ is shown in Fig. 5. The main difference from the compensated barrier case (Fig. 2) is that the parity of the P and AP configurations is interchanged. The reason is that for an odd number of magnetic layers the interface magnetic moments are parallel, instead of antiparallel, which interchanges the symmetry of the P and AP configurations. ME-TER is an odd function of the bias in the AP configuration passing through the origin at zero bias, and an even function in the P configuration displaying a finite value at zero voltage. Switching of the AFM order parameter in the AP configuration produces two equivalent states, ↓|↑...↑|↑ and ↓|↓...↓|↑. On the contrary, in the P configuration the ME switching implies a transition between two distinct states, ↑|↑...↑|↑ and ↑|↓...↓|↑, which is associated with a considerable change in the resistance and higher ME-TER values.

Another difference, in comparison with the compensated barrier case, is the more pronounced dependence of ME-TER on the barrier thickness. The values of ME-TER increase with the number of magnetic layers (Fig. 5), which suggests that the effect is not purely interfacial. Due to the lack of polarization, this effect can only be attributed to spin filtering in the bulk of the barrier due to the non-zero net magnetization. This also leads to stronger dependence of the ME-TER effect on the bias.

D. D. Uncompensated barriers with finite polarization

Finally, we consider uncompensated ME-MF barriers exhibiting both AFM and FE orders. The voltage behavior of the TER for the corresponding MFTJs is plotted in Fig. 6. The graphs can again be interpreted as a result of the superposition of the ME-TER effect associated with AFM order switching and the conventional FE-TER effect due to the screening of polarization charges in the electrodes, except that in this case the additional effect of spin filtering is evident from the thickness dependence of TER. The ME-TER and FE-TER effects in the P configuration have opposite parity, breaking the symmetry

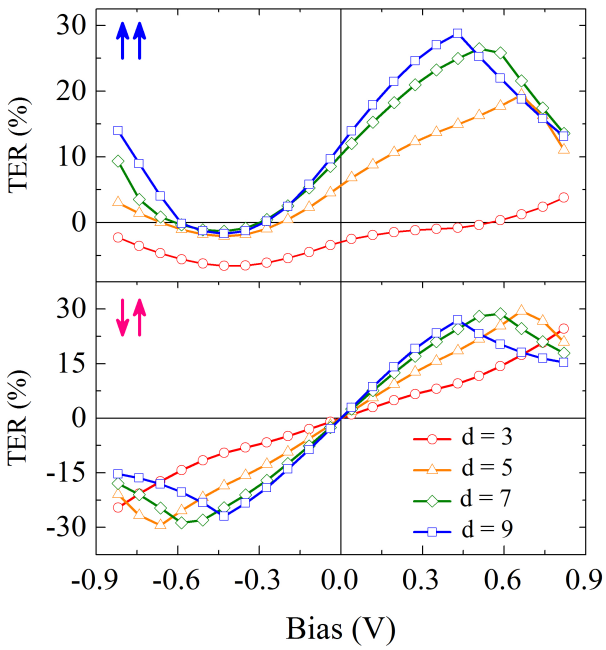

FIG. 6: Bias dependence of TER in MFTJs with P (top) and AP (bottom) alignment of the FM electrodes. The number of magnetic layers in the uncompensated barriers varies from 3 to 9 monolayers. The FE polarization is set to $P = 30\mu C/cm^2$.

of the TER curve.

IV. IV. SUMMARY AND CONCLUSIONS

We predict the existence of a ME-TER effect in MFTJs with ME-AFM barriers, arising from the switching of the AFM order parameter with applied electric field by means of the ME coupling. The effect is highly tunable and it can be effectively turned on and off by an applied magnetic field. In ME-MF barriers with non-vanishing FE polarization, we find a generalized TER effect which is a superposition of the ME-TER effect, due to the AFM order switching, and the conventional FE-TER effect, due to polarization screening. The electric-field control of the resistance in MFTJs provides a mostly dissipationless alternative to conventional TMR devices where high currents are required both for magnetic-field- and spin-torque-induced magnetization switching. Furthermore, electric-field switching of the AFM order parameter in ME-AFM barriers offers a means to control the exchange coupling to adjacent FM electrodes. Hence, magnetization reversal of FM electrodes could be assisted by applied voltage, leading to lower power consumption, which is an added advantage over FE-TER and conventional TMR devices with passive barriers. Based on these results we expect that single-phase ME-AFM and ME-MF (FE-AFM) materials, when used as active barriers in MFTJs, could be conducive to novel non-volatile resistive memory concepts.

Acknowledgments

This work was supported by NSF (Grants Nos. EPS-1002410, EPS-1010094, and DMR-1105474). JV acknowledges the support of the University of Grenoble.

[1] E. Y. Tsymbal, O. N. Mryasov, and P. R. LeClair, Spin-dependent tunnelling in magnetic tunnel junctions, J. Phys.: Condens. Matter **15**, R109 (2003).
[2] J. C. Slonczewski, Current-driven excitation of magnetic multilayers, J. Magn. Mater. **159**, L1 (1996).
[3] L. Berger, Emission of spin waves by a magnetic multilayer traversed by a current, Phys. Rev. B **54**, 9353 (1996).
[4] E. Y. Tsymbal and H. Kohlstedt, Tunneling Across a Ferroelectric, Science **313**, 181 (2006).
[5] J. P. Velev, S. S. Jaswal, and E. Y. Tsymbal, Multi-ferroic and magnetoelectric materials and interfaces, Phil. Trans. R. Soc. A **369**, 3069 (2011).
[6] M. Y. Zhuravlev, R. F. Sabirianov, S. S. Jaswal, and E. Y. Tsymbal, Giant Electroresistance in Ferroelectric Tunnel Junctions, Phys. Rev. Lett. **94**, 246802 (2005).
[7] J. P. Velev, C.-G. Duan, K. D. Belashchenko, S. S. Jaswal, and E. Y. Tsymbal, Effect of Ferroelectricity on Electron Transport in Pt/$BaTiO_3$/Pt Tunnel Junctions, Phys. Rev. Lett. **98**, 137201 (2007).
[8] V. Garcia, S. Fusil, K. Bouzehouane, S. Enouz-Vedrenne, N. D. Mathur, A. Barthelemy, and M. Bibes, Giant tunnel electroresistance for non-destructive readout of ferroelectric states, Nature **460**, 81 (2009).
[9] P. Maksymovych, S. Jesse, P. Yu, R. Ramesh, A. P. Baddorf, and S. V. Kalinin, Polarization Control of Electron Tunneling into Ferroelectric Surfaces, Science **324**, 1421 (2009).
[10] A. Gruverman, D. Wu, H. Lu, Y. Wang, H. W. Jang, C. M. Folkman, M. Ye. Zhuravlev, D. Felker, M. Rzchowski, C.-B. Eom, and E. Y. Tsymbal, Tunneling Electroresistance Effect in Ferroelectric Tunnel Junctions at the Nanoscale, Nano Lett. **9**, 3539 (2009).
[11] J. P. Velev, C.-G. Duan, J. D. Burton, A. Smogunov, M. Niranjan, E. Tosatti, S. Jaswal, and E. Tsymbal, Magnetic Tunnel Junctions with Ferroelectric Barriers: Prediction of Four Resistance States from First Principles, Nano Lett. **9**, 427 (2009).
[12] V. Garcia, M. Bibes, L. Bocher, S. Valencia, F. Kronast, A. Crassous, X. Moya, S. Enouz-Vedrenne, A. Gloter, D. Imhoff et al., Ferroelectric Control of Spin Polarization, Science **327**, 1106 (2010).

[13] S. Valencia, A. Crassous, L. Bocher, V. Garcia, X. Moya, R. O. Cherifi, C. Deranlot, K. Bouzehouane, S. Fusil, A. Zobelli et al., Interface-induced room-temperature multiferroicity in $BaTiO_3$, Nat. Mater. **10**, 753 (2011).

[14] D. Pantel, S. Goetze, D. Hesse, and M. Alexe, Reversible electrical switching of spin polarization in multiferroic tunnel junctions, Nat. Mater. **11**, 289 (2012).

[15] D. I. Khomskii, Classifying multiferroics: Mechanisms and effects, Physics **2**, 20 (2009).

[16] M. Gajek, M. Bibes, A. Barthélémy, K. Bouzehouane, S. Fusil, M. Varela, J. Fontcuberta, and A. Fert, Spin filtering through ferromagnetic $BiMnO_3$ tunnel barriers, Phys. Rev. B **72**, 020406(R) (2005).

[17] M. Gajek, M. Bibes, S. Fusil, K. Bouzehouane, J. Fontcuberta, A. Barthélémy and A. Fert, Tunnel junctions with multiferroic barriers, Nat. Mater. **6**, 296 (2007).

[18] M. Fiebig, Revival of the magnetoelectric effect, J. Phys. D. Appl. Phys. **38**, R123 (2005).

[19] J.-P. Rivera, A short review of the magnetoelectric effect and related experimental techniques on single phase (multi-) ferroics, Eur. Phys. J. B **71**, 299 (2009).

[20] A. Iyama and T. Kimura, Magnetoelectric hysteresis loops in Cr_2O_3 at room temperature, Phys. Rev. B **87**, 180408 (2013).

[21] P. Borisov, A. Hochstrat, X. Chen, W. Kleemann, and C. Binek, Magnetoelectric Switching of Exchange Bias, Phys. Rev. Lett. **94**, 117203 (2005).

[22] X. He, Y. Wang, N. Wu, A. N. Caruso, E. Vescovo, K. D. Belashchenko, P. A. Dowben and C. Binek, Robust isothermal electric control of exchange bias at room temperature, Nat. Mater. **9**, 579 (2010).

[23] T. Ashida, M. Oida, N. Shimomura, T. Nozaki, T. Shibata and M. Sahashi, Isothermal electric switching of magnetization in Cr_2O_3/Co thin film system, Appl. Phys. Lett. **106**, 132407 (2015).

[24] A. Sokolov, C.-S. Yang, E. Ovtchenkov, L. Yuan, S.-H. Liou and B. Doudin, Bistable memory effect in chromium oxide junctions, Mater. Res. Soc. Symp. Proc. **746**, 139 (2003).

[25] C. Binek and B. Doudin, Magnetoelectronics with magnetoelectrics, J. Phys.: Condens. Matter **17**, L39 (2004).

[26] W. Ratcliff, Z. Yamani, V. Anbusathaiah, T. R. Gao, P. A. Kienzle, H. Cao, and I. Takeuchi, Electric-field-controlled antiferromagnetic domains in epitaxial $BiFeO_3$ thin films probed by neutron diffraction, Phys. Rev. B **87**, 140405R (2013).

[27] S. M. Wu, S. A. Cybart, D. Yi, J. M. Parker, R. Ramesh, and R. C. Dynes, Full Electric Control of Exchange Bias, Phys. Rev. Lett. **110**, 067202 (2013).

[28] C. Binek, Controlling Magnetism with a Flip of a Switch, Physics **6**, 13 (2013).

[29] R. Ramesh and N. Spaldin, Multiferroics: progress and prospects in thin films, Nat. Mater. **6**, 21-29 (2007).

[30] A. Useinov, A. Kalitsov, J. Velev and N. Kioussis, Bias-dependence of the tunneling electroresistance and magnetoresistance in multiferroic tunnel junctions, Appl. Phys. Lett. **105**, 102403 (2014).

[31] A. Useinov, A. Kalitsov, J. Velev, and N. Kioussis, Ferroelectric control of spin-transfer torque in multiferroic tunnel junctions, Phys. Rev. B **91**, 094408 (2015).

[32] S. Shi, A. L. Wysocki and K. D. Belashchenko, Magnetism of chromia from first-principles calculations, Phys. Rev. B **79**, 104404 (2009).

[33] J. B. Neaton, C. Ederer, U. V. Waghmare, N. A. Spaldin, and K. M. Rabe, First-principles study of spontaneous polarization in multiferroic $BiFeO_3$, Phys. Rev. B. **71**, 014113 (2009).

[34] M. Y. Zhuravlev, S. Maekawa, and E. Y. Tsymbal, Effect of spin-dependent screening on tunneling electroresistance and tunneling magnetoresistance in multiferroic tunnel junctions, Phys. Rev. B **81**, 104419 (2010).

[35] A. Kalitsov, W. Silvestre, M. Chshiev, and J. Velev, Spin torque in magnetic tunnel junctions with asymmetric barriers, Phys. Rev. B **88**, 104430 (2013).

[36] Switching is governed by the product EH, rather than by E alone. EH products of (1kV/mm).(154mT) were used to achieve isothermal ME switching of a single crystal of chromia at room temperature [22]. Isothermal ME switching has been recently observed at low temperature in 500-nm-thick chromia films applying products $EH =$ (160kV/mm)·(6kOe) [23].

[37] X.-G. Zhang and W. H. Butler, Band structure, evanescent states, and transport in spin tunnel junctions, J. Phys.: Condens. Matter **15** R1603 (2003).

[38] K. D. Belashchenko, E. Y. Tsymbal, M. van Schilfgaarde, D. A. Stewart, I. I. Oleynik, and S. S. Jaswal, Effect of interface bonding on spin-dependent tunneling from the oxidized Co surface, Phys. Rev. B **69**, 174408 (2004).

[39] A. Kalitsov, P-J. Zermatten, F. Bonell, G. Gaudin, S. Andrieu, C. Tiusan, M. Chshiev and J. Velev, Bias dependence of tunneling magnetoresistance in magnetic tunnel junctions with asymmetric barriers, J. Phys. Condens. Matter **49**, 496005 (2013).

[40] Electric fields of 20 kV/mm have been used to switch AFM domains in 1000 nm-thick epitaxial films of BFO via the ME coupling [26]. Likewise, AFM order parameter switching has been achieved at low temperature in 200 nm-thick epitaxial layers of BFO with electric fields of the order of 120 kV/mm (i.e., ± 24 V voltage pulses applied between the 200 nm BFO layer and a 3 nm LSMO layer acting as conducting channel) [27].